Supplement for

Iron Oxide Inclusions and Exsolution Textures of Rainbow Lattice Sunstone

Shiyun Jin[1], Ziyin Sun[1], Aaron C. Palke[1]

[1]Gemological Institute of America, 5355 Armada Drive, Carlsbad, California 92008, U.S.A.

Correspondence to: Shiyun Jin (sjin@gia.edu)

Table S1. Trace element concentrations in the RLS in ppmw. The detection limit (dl) of each element is provided below the element symbol.

	Li *0.06*	**Mg** *0.05*	**P** *2.82*	**Sc** *0.04*	**Ti** *0.20*	**Mn** *0.07*	**Fe** *1.22*	**Ga** *0.01*	**Ge** *0.12*	**Rb** *0.01*
1	1.54	16.8	218	3.66	32.4	3.39	108	8.76	1.15	224
2	0.50	19.7	220	3.74	33.2	3.40	131	8.57	1.45	222
3	0.32	12.3	222	3.63	33.0	3.27	200	8.90	1.28	223
4	0.47	20.3	213	3.72	33.5	3.48	121	8.69	1.28	226
5	0.60	16.1	295	3.71	35.3	4.77	97	7.40	1.72	217
6	0.67	17.7	294	3.69	34.4	5.25	131	7.36	1.56	219
7	1.36	23.1	287	3.10	43.0	6.77	154	8.29	1.61	263
8	1.09	20.8	301	2.99	42.1	6.21	129	7.81	1.58	267
9	0.57	22.5	292	3.12	41.5	10.5	189	7.49	1.62	267
10	1.02	20.5	300	3.03	43.3	6.20	113	7.77	1.67	269
Ave.	0.81	19.0	264	3.44	37.2	5.33	137	8.11	1.49	240
	Sr *0.03*	**Y** *0.001*	**Cs** *0.08*	**La** *0.001*	**Ce** *0.005*	**Pr** *0.002*	**Nd** *0.002*	**Eu** *0.001*	**Tl** *0.002*	**Pb** *0.04*
1	842	0.049	0.42	4.25	3.52	0.184	0.330	2.61	1.06	98
2	894	0.049	0.40	4.35	3.34	0.134	0.243	2.70	1.11	101
3	727	0.037	0.38	7.65	3.37	0.158	0.304	2.20	1.12	85
4	847	0.049	0.41	4.56	4.04	0.231	0.498	2.59	1.09	94
5	749	0.071	0.39	3.92	3.56	0.207	0.438	2.59	1.07	103
6	816	0.087	0.36	3.75	5.58	0.144	0.361	2.83	1.09	113
7	801	0.103	0.48	4.83	4.02	0.220	0.367	3.10	0.77	119
8	803	0.093	0.50	4.70	3.69	0.187	0.245	3.37	0.81	117
9	767	0.096	0.47	4.26	3.19	0.140	0.230	3.18	0.79	113
10	799	0.088	0.48	4.81	4.26	0.237	0.420	3.13	0.84	117
Ave.	804	0.072	0.43	4.71	3.86	0.184	0.344	2.83	0.98	106

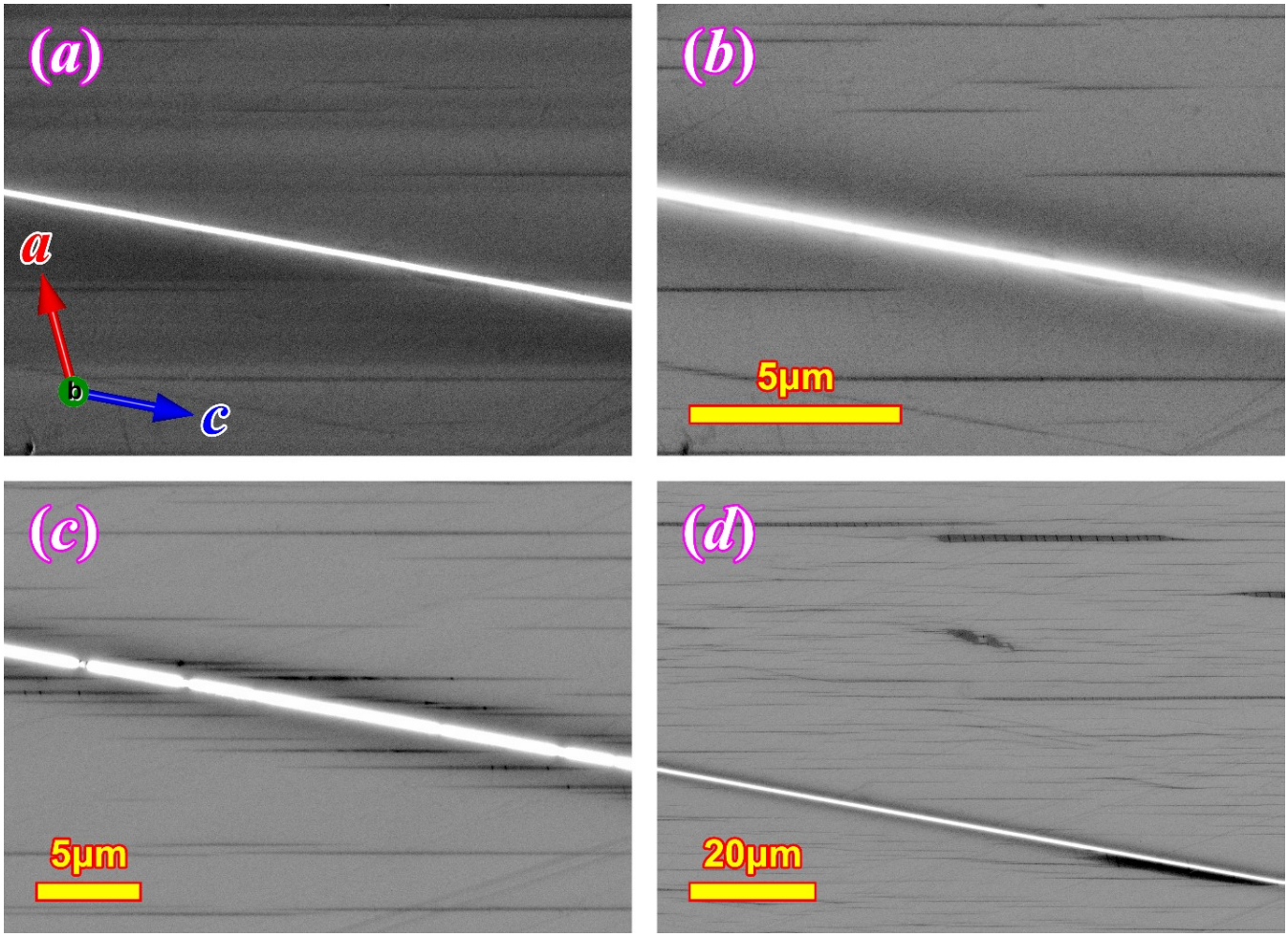

Figure S1: The iron oxide film inclusions parallel to (100) plane in the RLS under SEM. (*a*) and (*b*) are the secondary electron (SE) image and backscattered electron (BSE) image of the same area. The SE image shows sharp boundaries between the inclusion and the feldspar matrix, and reflect the thickness of the iron oxide film more accurately. The iron oxide film is ~100 nm in (*a*). The BSE images in (*b*), (*c*) and (*d*) shows a halo with gradual brightness change, making the film appear much thicker than they actually are (at least twice depending on the adjusted brightness and contrast). The albite films would terminate before they reach the iron oxide film (*c*), and some oligoclase spindles with tilted orientation can be found attached to the oxide film (*b*), similar to Fig. 5*d*.

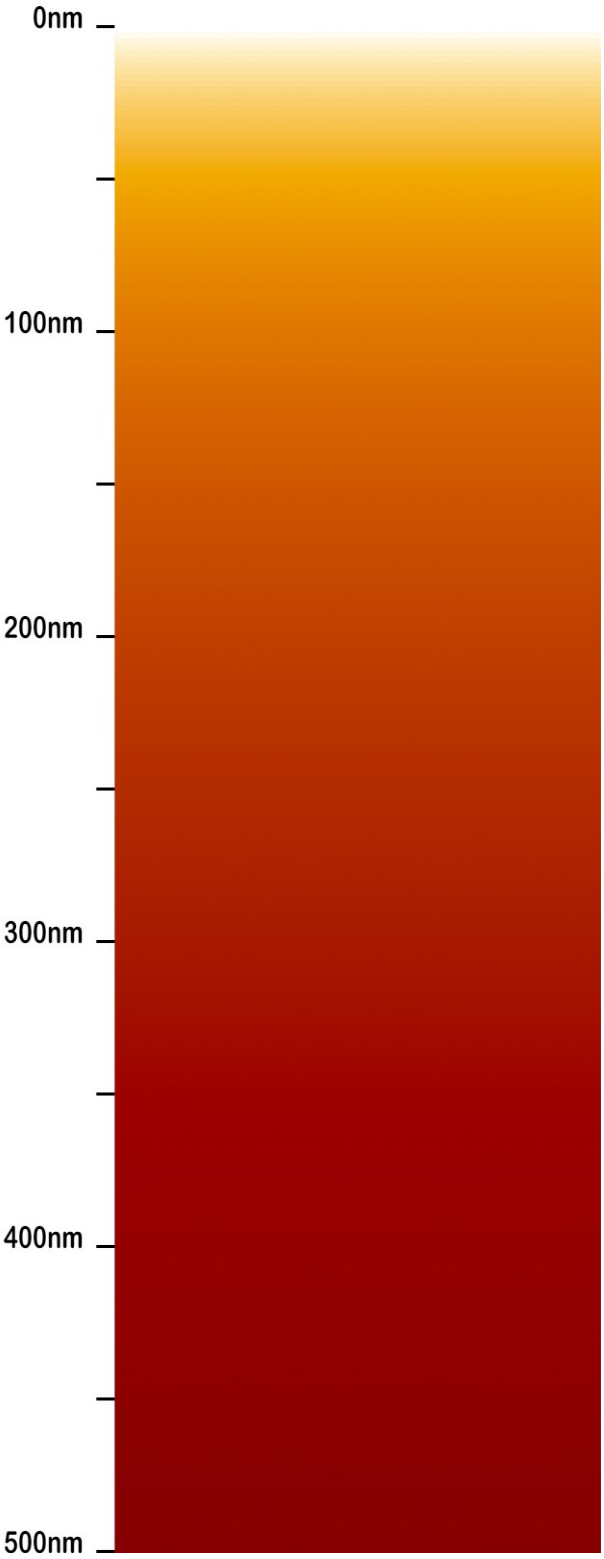

Figure S2: The calculated color of hematite films with increasing thickness, using the equations by Sun et al. (2017) with the absorption spectrum from Marusak et al. (1980). Under reflected light, the body color of hematite is totally overshadowed by the brilliant interference color (the "rainbow" color in Fig. 1*a*), which can range from red to blue depending on the thickness of the crystal. The relationship between the wavelength of the interference color (λ) and the thickness of the hematite crystal (d) is: $2n_{Hm}d\sin\theta = (m-½)\lambda$, in which the -½λ is from the 180° phase shift of the reflection on the top surface of the inclusion. With θ=90°, n_{Hm}≈3, a hematite inclusion displaying blue interference color (λ~480nm) would be ~40nm thick if m=1, and ~120nm for m=2, agreeing with the yellow body color (Fig. 4*a*).

Sun, Z., Palke, A. C., Muyal, J., and Mcmurtry, R.: How to facet gem-quality chrysoberyl: Clues from the relationship between color and pleochroism, with spectroscopic analysis and colorimetric parameters, Am. Mineral., 102, 1747–1758, https://doi.org/10.2138/am-2017-6011, 2017.

Marusak, L. A., Messier, R., and White, W. B.: Optical absorption spectrum of hematite, αFe_2O_3 near IR to UV, J. Phys. Chem. Solids, 41, 981–984, https://doi.org/10.1016/0022-3697(80)90105-5, 1980.

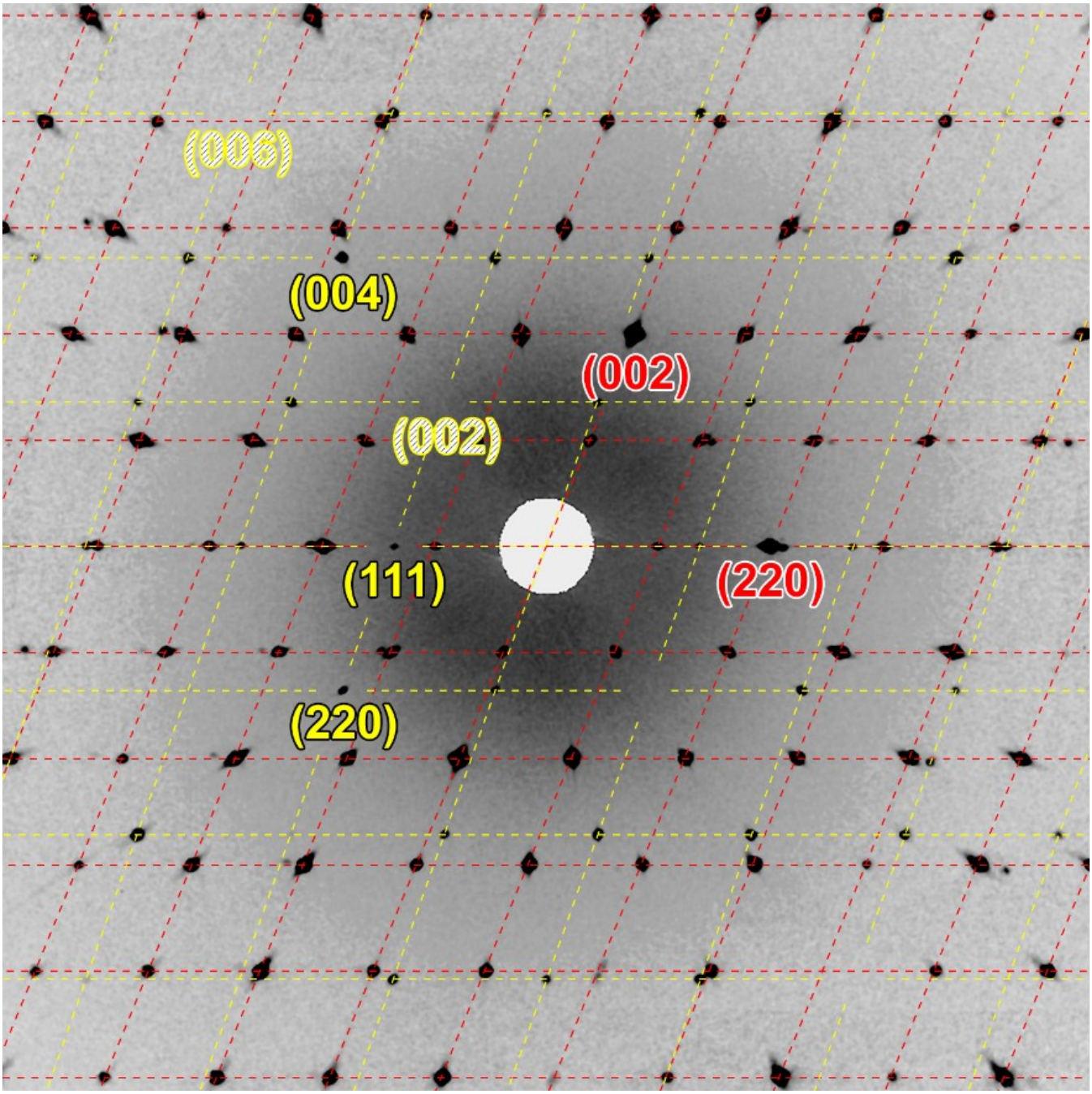

Figure S3: The *hhl* precession image ($[1\bar{1}0]$ zone axis) of orthoclase (and the magnetite seed) from data collected on Crystal 2, showing a specific COR of $\{111\}_{Mt} \parallel \{110\}_{Or}$ and $\langle 1\bar{1}0\rangle_{Mt} \parallel \langle 1\bar{1}0\rangle_{Or}$ between the inclusion and the host. The labels and reciprocal lattices follow the same colors as in Fig. 6. This COR has not been reported for magnetite needles in plagioclase.

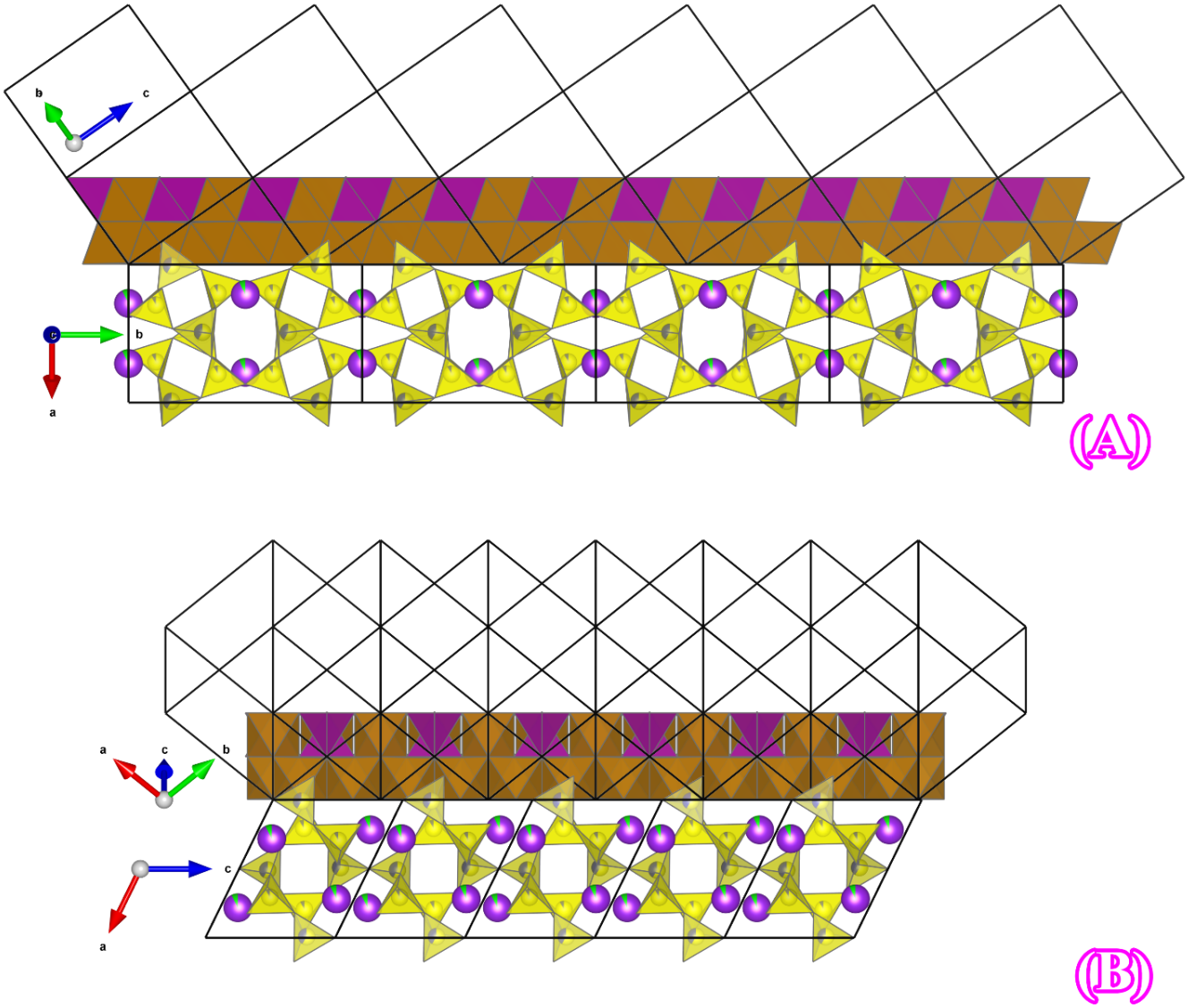

Figure S4 The structure relation between the orthoclase and magnetite film in the RLS. Note that this figure is only meant to illustrate the near perfect match in lattice dimensions between the two structures, and by no means represent the physical reality of the actual interface between the two phases.